Desalination and Water Treatment
www.deswater.com

doi: 10.5004/dwt.2017.20459

70 (2017) 347–354
April

Bi-amino surface functionalized nanoparticles: synthesis and binary system dye removal from wastewater containing anionic dyes

Niyaz Mohammad Mahmoodi[a,*], Mina Ghezelbash[b], Cyrus Ghotbei[b], Mohammad Kazemeini[b]

[a]*Department of Environmental Research, Institute for Color Science and Technology, Tehran, Iran, Tel. +98 021 22969771; Fax: +98 021 22947537; email: mahmoodi@icrc.ac.ir*
[b]*Department of Chemical & Petroleum Engineering, Sharif University of Technology, Tehran, Iran, emails: mina.ghezelbash@yahoo.com (M. Ghezelbash), ghotbi@sharif.edu (C. Ghotbei), kazemini@sharif.edu (M. Kazemeini)*

Received 8 September 2016; Accepted 25 December 2016

ABSTRACT

In this paper, copper oxide nanoparticle was synthesized, and its surface was modified using *N*-(2-aminoethyl)-3-(trimethoxysilyl)propylamine. The bi-amino surface functionalized nanoparticle (BASFN) was used to remove anionic dyes from single and binary systems. The scanning electron microscopy (SEM), Fourier transform infrared (FTIR) spectroscopy, energy-dispersive X-ray spectroscopy (EDAX) and X-ray diffraction were used to characterize the nanoparticle. Direct Red 80 (DR80) and Direct Green 6 (DG6) were used as anionic dyes. The effect of adsorbent dosage, dye concentration and pH on dye removal was evaluated. Kinetic of dye adsorption on BASFN followed pseudo-second order. The results showed that the experimental data were correlated reasonably well by Langmuir and Freundlich isotherm in single and binary system, respectively. The maximum dye adsorption capacity (Q_0) of BASFN was 217 and 250 mg/g for DR80 and DG6, respectively.

Keywords: Synthesis; Nanoparticle; Surface functionalization; Binary system dye removal; Wastewater

1. Introduction

The environmental problems of industrial activities have gained much attention over the years. Industries consume more and more water but water supply is not increased. This is a global concern. Color due to the presence of dyes in water and wastewater is the first contaminant to be recognized and undesirable. Nowadays, commercial dyes with more than one hundred thousand kinds are produced over nine million tons annually. The anionic dyes of effluents are of serious concern because of their adverse effects on human beings and environment. The chemical stability of dyes causes low dye removal efficiency by traditional wastewater treatment processes [1–14].

The selection of an appropriate dye removal treatment process needs to know the composition of wastewater. It causes to improve the quality of the discharged treated wastewater into the ecosystem. The several operational variables, economics and local standards should be investigated to choose the best treatment process. Various technologies including adsorption, advanced oxidation processes, filtration etc. were studied to remove pollutants from wastewater. These methods have some limitations while they have been widely used. Depending on the kinds of adsorbent, adsorption technologies represent one of the most efficient and cheap alternatives toward the treatment of wastewater, which may contain several kinds of pollutants like dyes. Adsorption process has many advantages including the cost effectiveness, simplicity of operation, easy regeneration, high efficiency and sludge-free operation, but it has some limitations such as a relatively low adsorption

* Corresponding author.

capacity for organic pollutants. Thus, researchers are focusing on novel adsorbents [15–20].

The health, energy and water as fundamental issues can be addressed by nanotechnology. The nanomaterials could supply an influential platform for separation, catalysis, sensing etc. because of their large specific surface area and the high affinity toward target compounds by functionalization with different active compounds [21–23].

A literature review showed that the functionalized copper oxide nanoparticle with *N*-(2-Aminoethyl)-3-(trimethoxysilyl) propylamine was not investigated to adsorb anionic dyes from binary system dye removal. In this paper, copper oxide nanoparticle was synthesized and functionalized using *N*-(2-Aminoethyl)-3-(trimethoxysilyl)propylamine. The characteristics of the bi-amino surface functionalized nanoparticle (BASFN) were investigated using Fourier transform infrared (FTIR), X-ray diffraction (XRD), scanning electron microscopy (SEM) and energy-dispersive X-ray spectroscopy (EDAX). Direct Green 6 (DG6) and Direct Red 80 (DR80) were used as model dyes. The dependency of adsorption performances to effective variables including adsorbent dosage, initial dye concentration and pH was systematically studied. The kinetic and isotherm of dye adsorption were studied.

2. Materials and methods

2.1. Chemicals

DR80 and DG6 were obtained from Ciba and used without further purification. The chemical structure of dyes was shown in Fig. 1. All other chemicals were of analytical grade and obtained from Merck (Germany).

2.2. Synthesis of the nanomaterials

2.2.1. Synthesis of copper oxide nanoparticle

1 g of $CuSO_4.5H_2O$ and 1 g of NaOH were dissolved under stirring in 90 mL of distilled water. The mixed solution was sealed in a glass bottle and kept static at 120°C for 24 h, and then cooled to room temperature naturally. The final precipitate was washed with distilled water several times to remove the possible residues and then dried at 120°C for 12 h.

2.2.2. Synthesis of bi-amino surface functionalized nanoparticle (BASFN)

1 g of CuO and 1.5 mL of *N*-(2-aminoethyl)-3-(trimethoxysilyl)propylamine were poured into toluene and refluxed for 24 h. The precipitate was filtered, washed with toluene and deionized water, and dried.

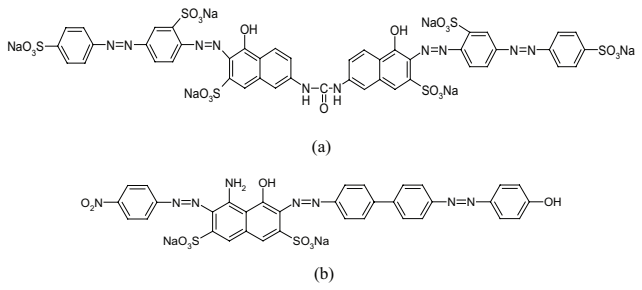

Fig. 1. The chemical structure of dyes: (a) DR80 and (b) DG6.

2.3. Physicochemical characterization

The functional groups of material were studied by FTIR spectrum (PerkinElmer Spectrophotometer Spectrum One) in the range of 4,000–450 cm^{-1}. Crystallization behavior was identified by XRD model Siemens D-5000 diffractometer with Cu Kα radiation (λ = 1.5406Å) at room temperature. The morphological structure of the material was examined by SEM using a LEO 1455VP scanning microscope. EDAX analysis were conducted using Noran system SIX model energy dispersive X-ray microanalysis system (Thermo Electron Corporation, Japan) attached to SEM.

2.4. Adsorption procedure

The batch adsorption technique was used to study the effect of various process variables such as adsorbent dosage, initial dye concentration and pH on adsorption. The dye adsorption measurements were done by mixing various adsorbent dosages (0.0125–0.075 g) in jars containing 250 mL of dye solution (50 mg/L). Dye solutions were prepared using distilled water to prevent and minimize possible interferences. Experiments were carried out at 25°C for 60 min to attain equilibrium conditions. The solution pH was adjusted by adding a small amount of H_2SO_4 or NaOH. At the end of dye adsorption process, samples were centrifuged, and their absorbance was determined. The changes of absorbance were determined at certain time intervals (2.5, 5, 7.5, 10, 15, 20, 30, 40, 50 and 60 min) during the adsorption process using UV–Vis PerkinElmer Lambda 25 spectrophotometer. The maximum wavelength (λ_{max}) of DG6 and DR80 to determine residual dye concentration in solution was 633 and 543 nm, respectively.

The kinetic and isotherm of dye adsorption were studied by contacting 250 mL of dye solution with initial dye concentration of 50 mg/L and pH 2.1 at room temperature (25°C) for 60 min at different adsorbent dosages (0.0125–0.075 g).

The effect of adsorbent dosage (0.0125–0.075 g) on dye removal was investigated by contacting 250 mL of dye solution with initial dye concentration of 50 mg/L at room temperature (25°C) for 60 min and pH 2.1.

The effect of initial dye concentration (50, 100, 150 and 200 mg/L) on dye removal was investigated by contacting 250 mL of dye solution with adsorbent at room temperature (25°C) for 60 min and pH 2.1.

The effect of pH (2.1, 5, 8 and 11) on dye removal was investigated by contacting 250 mL of dye solution with 50 mg/L initial dye concentration at room temperature (25°C) for 60 min.

3. Results and discussion

3.1. Characterization

The FTIR spectrum of copper oxide nanoparticle was shown in Fig. 2. It has two peaks at 3,450 cm^{-1} and 600–500 cm^{-1}, which indicate O–H stretching vibration and metal-oxygen vibration, respectively. The peak at 1,625 cm^{-1} was attributed

to OH bending of molecular water. The FTIR spectrum of the BASFN displays a number of characteristic bands at 3,435, 2,883 and 2,822 cm^{-1}, and 600–500 cm^{-1} (Fig. 2). These bands are assigned to O–H and N–H stretching vibration, $–CH_2–$ vibration, and metal-oxygen vibration, respectively. The bending vibration of N–H (amine) and C–N (amine) display a strong band at 1,600–1,560 cm^{-1} and 1,350–1,000 cm^{-1}, respectively [24].

Fig. 3 illustrates the XRD pattern of the copper oxide nanoparticle and BASFN. All diffraction peaks in Fig. 3 are in good agreement with those of the standard pattern of monoclinic copper oxide (JCPDS (Joint Committee on Powder Diffraction Standards) Card No. 05-0661) [25].

SEM is used to determine the particle shape and size distribution of the material. The SEM micrographs of the copper oxide nanoparticle and the bi-amino surface functionalized copper oxide nanoparticle (Fig. 4) showed a relatively homogeneous nanoparticle size distribution. In addition copper oxide nanoparticle was not aggregated after surface functionalization process.

EDAX analysis (Fig. 5) showed that copper oxide nanoparticle contained 53.51% of Cu and 46.49% O before modification; and 11.49% C, 38.62% O, 5.69% N, 6.26% Si, and 37.93% Cu after modification. Thus, the results indicated that copper oxide nanoparticle was modified by amino functional group.

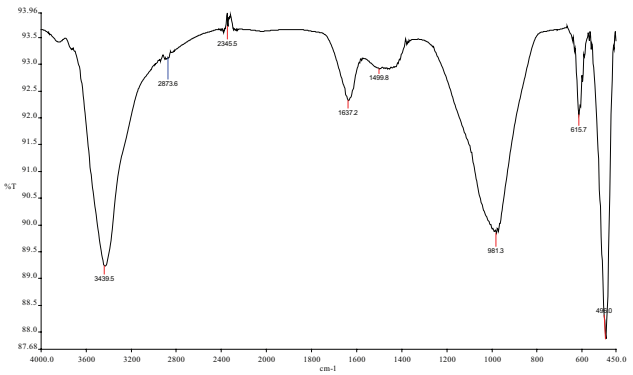

Fig. 2. FTIR spectrum of the synthesized nanoparticles: (a) copper oxide and (b) BASFN.

3.2. Adsorption kinetic and isotherm

The adsorption kinetics controls the adsorbate residence time and reactor dimensions. As a result, predicting the rate at which adsorption takes place for a given system is probably the most important factor in adsorption system design. The previous works of adsorption kinetics of dye removal revealed that the majority of the dyes were removed within the first 60 min of contact with the adsorbent [26–29]. Three kinetics models (intraparticle diffusion, pseudo-second order and pseudo-first order) were utilized to test the experimental data and predict the controlling mechanism of the dye adsorption.

Linear form of pseudo-first-order model is [26]:

$$\log(q_e - q_t) = \log(q_e) - (k_1/2.303)t \quad (1)$$

The linear fit between the $\log(q_e - q_t)$ and contact time (t) can be approximated as pseudo-first-order kinetics.

Linear form of pseudo-second-order model was illustrated as [27]:

$$t/q_t = 1/k_2 q_e^2 + (1/q_e)t \quad (2)$$

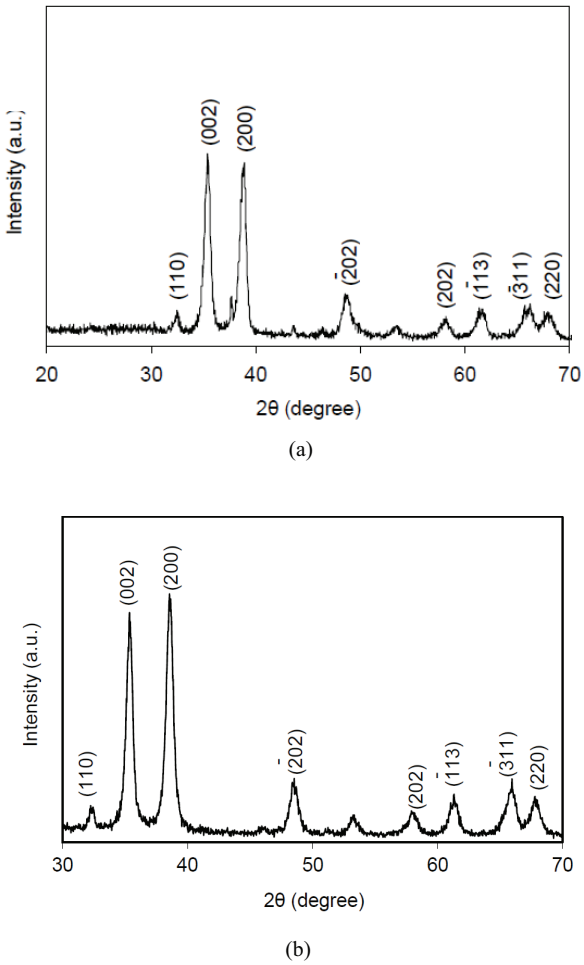

Fig. 3. XRD pattern of the synthesized nanoparticles: (a) copper oxide and (b) BASFN.

The possibility of intraparticle diffusion resistance affecting adsorption was investigated by the intraparticle diffusion model as [29]:

$$q_t = k_p t^{1/2} + I \quad (3)$$

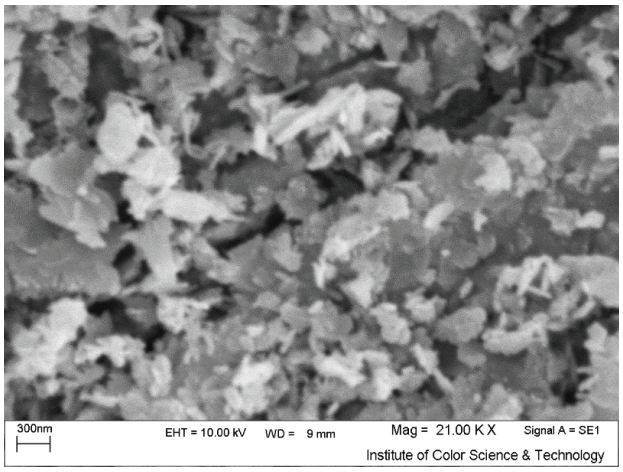

(a)

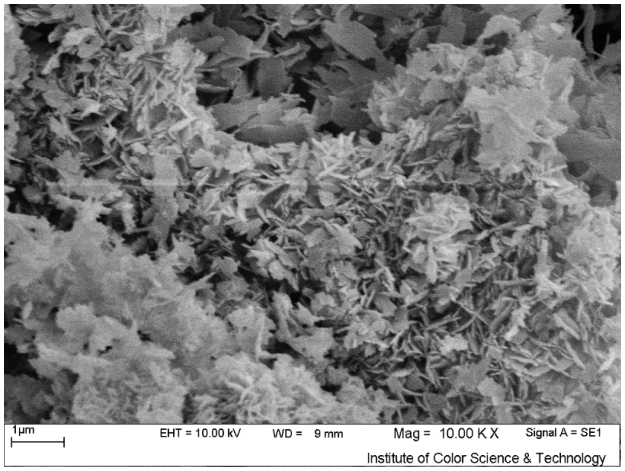

(b)

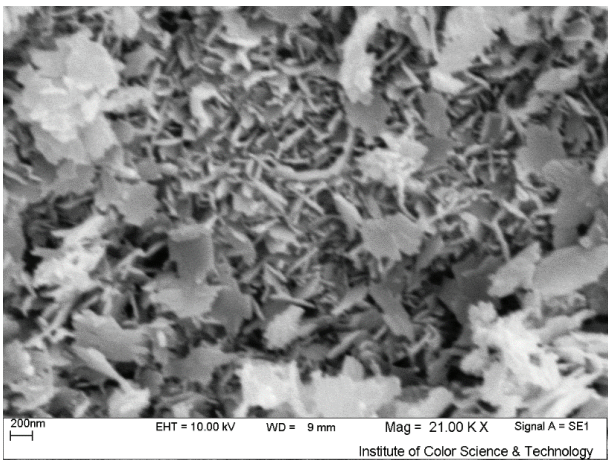

(c)

Fig. 4. SEM images of the synthesized nanoparticles: (a) copper oxide, and (b) and (c) BASFN.

In this research, the pseudo-first-order, pseudo-second-order and intraparticle diffusion models were used to study the dye adsorption kinetics at different adsorbent dosages. The kinetics constant values were shown in Table 1. The linearity of the plots (R^2) demonstrated that pseudo-first-order and intraparticle diffusion kinetic models did not play a significant role in the uptake of dye (Table 1). The linear fit and the R^2 values for pseudo-second-order kinetics model showed that the dye removal kinetic followed pseudo-second-order kinetics (Table 1). Also, the experimental values of q_e agreed with the calculated ones.

In order to optimize the adsorption mechanism pathways, it is important to establish the most appropriate correlation for the equilibrium curve [21,29]. Several isotherms such as the Langmuir, Freundlich and Temkin models were studied in detail.

The Langmuir equation describes monolayer adsorption. This model assumes a single layer of adsorbed pollutant at a constant temperature and a uniform energy of adsorption [30,31]. The Langmuir model is the most frequently employed model and is given by [28]:

$$C_e/q_e = 1/K_L Q_0 + C_e/Q_0 \quad (4)$$

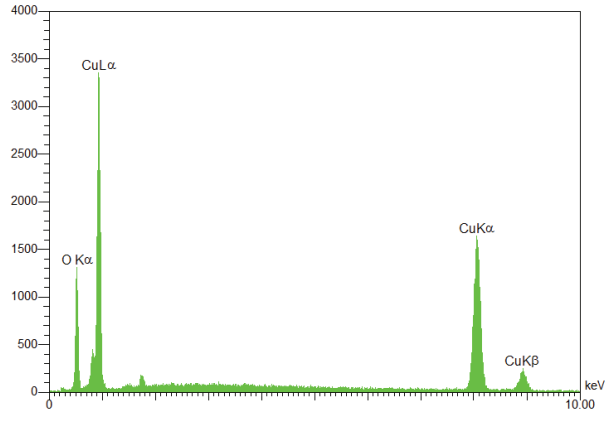

(a)

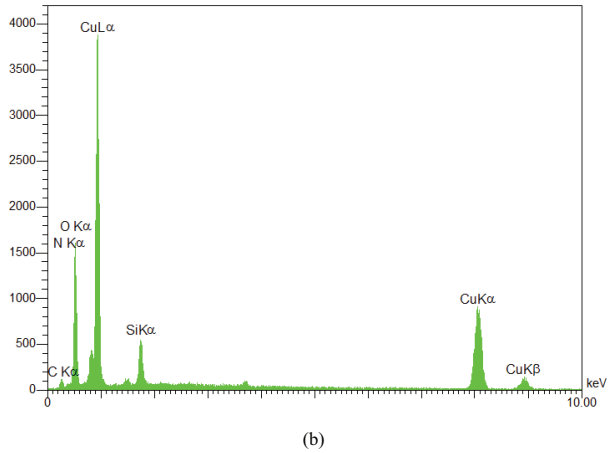

(b)

Fig. 5. EDAX pattern of the synthesized nanoparticles: (a) copper oxide and (b) BASFN.

Also, isotherm data were tested with the Freundlich isotherm that can be expressed by [32]:

$$\log q_e = \log K_F + (1/n)\log C_e \quad (5)$$

Temkin and Pyzhev suggested that due to the indirect adsorbate/adsorbent interaction, the heat of adsorption of all the molecules in the layer would decrease linearly with coverage. The Temkin isotherm is given as [33]:

$$Q_e = B_1 \ln K_T + B_1 \ln C_e \quad (6)$$

In this paper, the Langmuir, Freundlich and Temkin isotherms were used to investigate the dye adsorption isotherm at different adsorbent dosages. The isotherm constants values were shown in Table 2. The correlation coefficient values showed that the dye removal isotherm followed the Langmuir isotherm in single systems, while dye removal in binary system followed the Freundlich isotherm due to the interaction of dyes during adsorption process.

Table 1
Linearized kinetic coefficients for dye adsorption onto BASFN at different adsorbent dosages for single and binary systems

Dye	Adsorbent (g)	$(q_e)_{Exp}$	Pseudo-first order			Pseudo-second order			Intraparticle diffusion		
			$(q_e)_{Cal}$	k_1	R^2	$(q_e)_{Cal}$	k_2	R^2	k_p	I	R^2
Single system											
DR80	0.0125	201.333	140.281	0.0713	0.942	217.391	0.0008	0.998	24.471	41.284	0.847
	0.0250	184.000	117.571	0.0557	0.936	196.078	0.0009	0.997	21.342	40.081	0.842
	0.0500	148.077	92.087	0.0755	0.940	158.730	0.0015	0.998	17.085	38.911	0.787
	0.0750	147.273	73.080	0.0799	0.955	151.515	0.0028	0.999	14.710	55.827	0.698
DG6	0.0125	237.143	200.632	0.0488	0.966	294.118	0.0002	0.987	31.760	8.519	0.945
	0.0250	229.167	187.025	0.0705	0.917	294.118	0.0002	0.958	32.625	12.612	0.868
	0.0500	188.841	158.052	0.0769	0.961	227.273	0.0004	0.988	25.895	18.089	0.886
	0.0750	159.307	103.229	0.0843	0.944	175.439	0.0011	0.996	19.698	35.244	0.796
Binary system											
DR80 + DG6											
DR80	0.0125	220.339	17.140	0.0279	0.913	270.270	0.0003	0.983	29.968	21.230	0.893
	0.0250	187.943	14.632	0.0493	0.937	217.391	0.0006	0.984	24.261	29.434	0.840
	0.0500	119.932	7.734	0.0412	0.721	129.870	0.0014	0.998	14.403	26.109	0.827
	0.0750	96.419	6.079	0.0449	0.749	100.000	0.0040	0.999	10.274	33.254	0.714
DG6	0.0125	142.061	93.670	0.0686	0.949	153.846	0.0013	0.999	16.821	32.205	0.836
	0.0250	128.906	65.599	0.0808	0.911	136.986	0.0022	0.997	14.637	38.674	0.714
	0.0500	111.959	67.530	0.0613	0.930	119.048	0.0017	0.999	13.090	26.289	0.823
	0.0750	0.411	44.709	0.0686	0.939	93.458	0.0039	0.999	9.289	31.675	0.736

Table 2
Linearized isotherm coefficients for dye adsorption onto BASFN at different adsorbent dosages for single and binary systems

System	Langmuir			Freundlich			Temkin		
	Q_0	K_L	R^2	K_F	n	R^2	K_T	B_1	R^2
Single system	DR80								
	217	0.189	0.958	108	6.757	0.652	43	20	0.646
	DG6								
	250	0.421	0.995	140	7.017	0.960	120	28	0.941
Binary system (DR80 + DG6)	DR80								
	345	0.027	0.682	1	0.698	0.953	14	215	0.944
	DG6								
	357	0.016	0.902	11	1.473	0.965	7	78	0.951

3.3. Effect of operational parameter on dye removal

The dye removal vs. time (min) at different dosages (g) by the unmodified copper oxide nanoparticle was shown in Fig. 6. In addition dye adsorption ability of the BASFN from single (sin.) and binary (bin.) systems was presented in Fig. 7. Higher percentage of adsorption with the increase of adsorbent dosage can be attributed to increase in surface area and the availability of more binding sites on the adsorbent. The increase in uptake with increase in adsorbent dosage may be due to overlapping of adsorption sites as a result of over-crowding of adsorbent particles [30]. The results

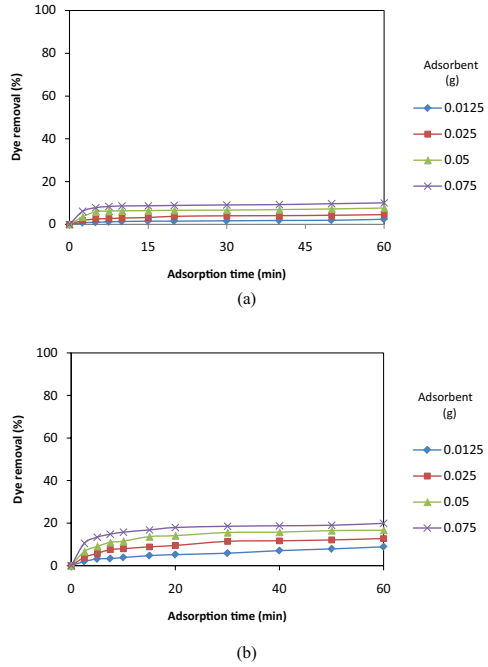

Fig. 6. The effect of adsorbent dosage (g) on dye removal by copper oxide from single system (dye concentration = 50 mg/L, pH = 2.1): (a) DR80 (sin.) and (b) DG6 (sin.).

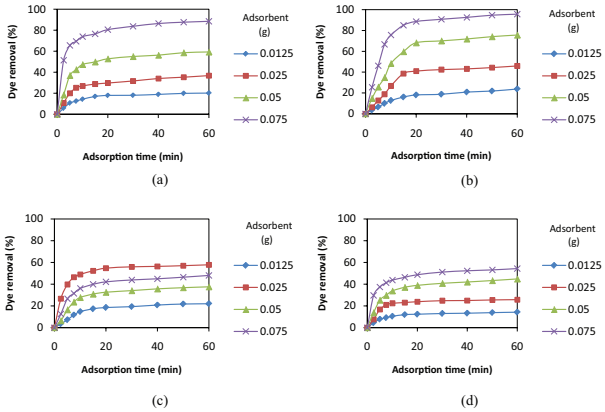

Fig. 7. The effect of adsorbent dosage (g) on dye removal by BASFN from single and binary systems (dye concentration = 50 mg/L, pH = 2.1): (a) DR80 (sin.), (b) DG6 (sin.), (c) DR80 (bin., DR80 + DG6) and (d) DG6 (bin., DR80 + DG6).

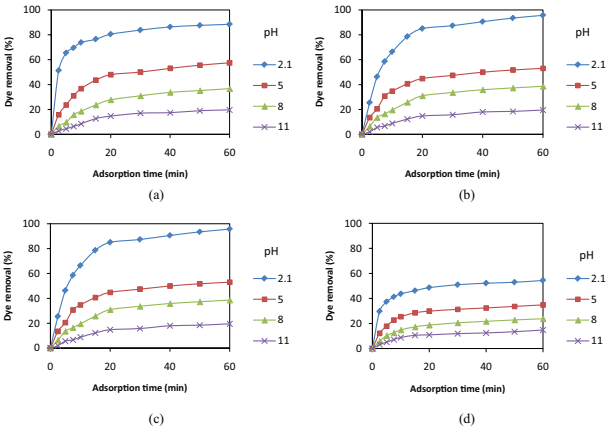

Fig. 8. The effect of pH on dye removal by BASFN from single and binary systems (dye concentration = 50 mg/L, adsorbent dosage = 0.075 g): (a) DR80 (sin.), (b) DG6 (sin.), (c) DR80 (bin., DR80 + DG6) and (d) DG6 (bin., DR80 +DG6).

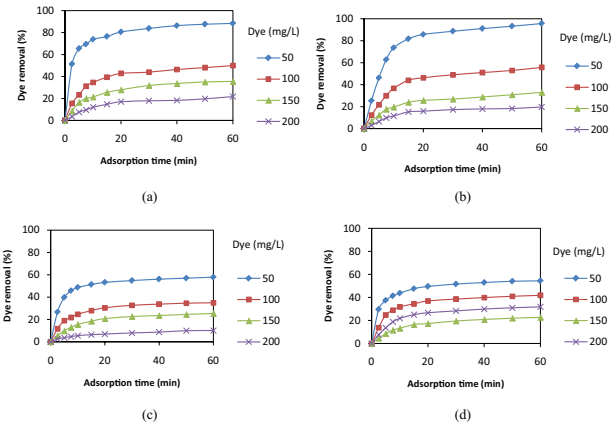

Fig. 9. The effect of dye concentration on dye removal by BASFN from single and binary systems (adsorbent dosage = 0.075 g, pH = 2.1): (a) DR80 (sin.), (b) DG6 (sin.), (c) DR80 (bin., DR80 + DG6) and (d) DG6 (bin., DR80 +DG6).

showed that dye removal ability of the BASFN is higher than that of the unmodified nanoparticle. Thus, BASFN was used as an adsorbent for further studies.

Amino functional groups of BASFN protonate at acidic pH, and the adsorption sites on adsorbent surface for anionic dye increase. Thus, dye removal increases by electrostatic attraction.

The pH of dye solution is of particular importance in analyzing the adsorption procedure and exploring the adsorption ability. The effect of pH on the adsorption of DR80 and DG6 in single and binary systems of dyes was shown in Fig. 8. At lower pH, more protons will be available to protonate amino groups of BASFN to form NH_3^+ groups, thereby increasing electrostatic attractions between negatively charged dye anions and positively charged adsorption sites and causing an increase in dye adsorption [28]. This explanation agrees with our data on pH effect. The maximum dye adsorption occurred at pH 2.1.

The effect of initial dye concentration of DR80 and DG6 in single and binary systems of dyes on the percentage of dye removal was studied. For both single and binary systems of dyes, the dye removal decreased with an increase in the initial concentrations as shown in Fig. 9. This might be due to the fact that at a fixed adsorbent dosage, the number of active adsorption sites to accommodate the adsorbate dye anions remained unchanged while with higher adsorbate concentration, the adsorbate anions to be accommodated increased. Thus, dye removal decreased [32,34].

4. Conclusions

In this paper, BASFN was synthesized and characterized. The dye removal ability of BASFN from single and binary systems was studied. DG6 and DR80 were used as anionic dyes. Dye adsorption capacity of the synthesized adsorbent (BASFN) for DG6 and DR80 was 250 and 217 mg/g, respectively. Adsorption kinetic of dyes was found to conform to pseudo-second-order kinetics for both single and binary systems. The equilibrium data was analyzed using the Langmuir, Freundlich and Temkin isotherms, and the characteristic parameters for each isotherm have been determined. The results showed that the experimental data were correlated reasonably well by Langmuir and Freundlich isotherm in single and binary system, respectively. It can be concluded that the synthesized adsorbent might be a suitable adsorbent to remove anionic dyes from colored wastewater.

Acknowledgment

This work was done in Department of Environmental Research, Institute for Color Science and Technology (ICST). Professor Mahmoodi is grateful for the support from the ICST.

Symbols

$1/n$	—	Adsorption intensity
B_1	—	Related to the heat of adsorption
C_e	—	Equilibrium concentration of dye solution, mg/L
I	—	Intercept
k_1	—	Equilibrium rate constant of pseudo-first-order kinetics, min^{-1}
k_2	—	Equilibrium rate constant of pseudo-second-order, g/mg min
K_F	—	Freundlich constant
K_L	—	Langmuir constant, L/g
k_p	—	Intraparticle diffusion rate constant
K_T	—	Equilibrium binding constant, L/mg
Q_0	—	Maximum adsorption capacity, mg/g
q_e	—	Amount of dye adsorbed at equilibrium, mg/g
$(q_e)_{Cal}$	—	The calculated q_e
$(q_e)_{Exp}$	—	The experimental q_e
q_t	—	Amount of dye adsorbed at time t, mg/g
R^2	—	Correlation coefficient values

References

[1] A. Bafana, S.S. Devi, T. Chakrabarti, Azo dyes: past, present and the future, Environ. Rev., 19 (2011) 350–370.
[2] N.M. Mahmoodi, Manganese ferrite nanoparticle: synthesis, characterization and photocatalytic dye degradation ability, Desal. Wat. Treat., 53 (2015) 84–90.
[3] G. Sharma, M. Naushad, D. Pathania, A. Mittal, G.E. El-desoky, Modification of *Hibiscus cannabinus* fiber by graft copolymerization: application for dye removal, Desal. Wat. Treat., 54 (2015) 3114–3121.
[4] A. Mittal, R. Ahmad, I. Hasan. Iron oxide-impregnated dextrin nanocomposite: synthesis and its application for the biosorption of Cr(VI) ions from aqueous solution, Desal. Wat. Treat., 57 (2016) 15133–15145.
[5] A. Mittal, Retrospection of Bhopal gas tragedy, Toxicol. Environ. Chem., 98 (2016) 1079–1083.
[6] N.M. Mahmoodi, Binary catalyst system dye degradation using photocatalysis, Fibers Polym., 15 (2014) 273–280.
[7] M. Uğurlu, Adsorption of a textile dye onto activated sepiolite, Microporous Mesoporous Mater., 119 (2009) 276–283.
[8] R. Wu, J. Qu, Y. Chen, Magnetic powder MnO–Fe_2O_3 composite—a novel material for the removal of azo-dye from water, Water Res., 39 (2005) 630–638.
[9] N.M. Mahmoodi, Synthesis of magnetic carbon nanotube and photocatalytic dye degradation ability, Environ. Monit. Assess., 186 (2014) 5595–5604.
[10] N.M. Mahmoodi, Magnetic ferrite nanoparticle–alginate composite: synthesis, characterization and binary system dye removal., J. Taiwan Inst. Chem. Eng., 44 (2013) 322–330.
[11] N.M. Mahmoodi, Photocatalytic ozonation of dyes using multiwalled carbon nanotube, J. Mol. Catal. A: Chem., 366 (2013) 254–260.
[12] N.M. Mahmoodi, Photodegradation of dyes using multiwalled carbon nanotube and ferrous ion, J. Environ. Eng., 139 (2013) 1368–1374.
[13] N.M. Mahmoodi, Photocatalytic degradation of dyes using carbon nanotube and titania nanoparticle, Water Air Soil Pollut., 224 (2013) 1612.
[14] N.M. Mahmoodi, N.Y. Limaee, M. Arami, S. Borhany, M. Mohammad-Taheri, Nanophotocatalysis using nanoparticles of titania: mineralization and finite element modelling of Solophenyl dye decolorization, J. Photochem. Photobiol., A, 189 (2007) 1–6.
[15] M.T. Vakili, M. Rafatullah, B. Salamatinia, A. Zuhairi Abdullah, M. Hakimi Ibrahim, K.B. Tan, Z. Gholami, P. Amouzgar, Application of chitosan and its derivatives as adsorbents for dye removal from water and wastewater: a review, Carbohydr. Polym., 113 (2014) 115–130.
[16] J. Fu, Q. Xin, X. Wu, Z. Chen, Y. Yan, S. Liu, M. Wang, Q. Xu, Selective adsorption and separation of organic dyes from aqueous solution on polydopamine microspheres, J. Colloid Interface Sci., 461 (2016) 292–304.
[17] A.A. Oladipo, M. Gazi, E. Yilmaz, Single and binary adsorption of azo and anthraquinone dyes by chitosan-based hydrogel: selectivity factor and Box-Behnken process design, Chem. Eng. Res. Des., 104 (2015) 264–279.
[18] L. Zhang, Y. Zeng, Z. Cheng, Removal of heavy metal ions using chitosan and modified chitosan: a review, J. Mol. Liq., 214 (2016) 175–191.
[19] M. Turabik, Adsorption of basic dyes from single and binary component systems onto bentonite: simultaneous analysis of Basic Red 46 and Basic Yellow 28 by first order derivative spectrophotometric analysis method, J. Hazard. Mater., 158 (2008) 52–64.
[20] N.M. Mahmoodi, Synthesis of core-shell magnetic adsorbent nanoparticle and selectivity analysis for binary system dye removal, J. Ind. Eng. Chem., 20 (2014) 2050–2058.
[21] G.Z. Kyzas, K.A. Matis, Nanoadsorbents for pollutants removal: a review, J. Mol. Liq., 203 (2015) 159–168.
[22] N.M. Mahmoodi, Nickel ferrite nanoparticle: synthesis, modification by surfactant and dye removal ability, Water Air Soil Pollut., 224 (2013) 1419.
[23] K.B. Tan, M.T. Vakili, B.A. Horri, P.E. Poh, A.Z. Abdullah, B. Salamatinia, Adsorption of dyes by nanomaterials: recent developments and adsorption mechanisms, Sep. Purif. Technol., 150 (2015) 229–242.

[24] D.L. Pavia, G.M. Lampman, G.S. Kaiz, Introduction to Spectroscopy: A Guide for Students of Organic Chemistry, W.B. Saunders Company, Philadelphia, 1987.
[25] B. Li, Y. Wang, Facile synthesis and photocatalytic activity of ZnO–CuO nanocomposite, Superlattices Microstruct., 47 (2015) 615–623.
[26] N.M. Mahmoodi, Z. Mokhtari-Shourijeh, Preparation of PVA–chitosan blend nanofiber and its dye removal ability from colored wastewater, Fibers Polym., 16 (2015) 1861–1869.
[27] Y.-S. Ho, Absorption of Heavy Metals from Waste Streams by Peat, PhD Thesis, University of Birmingham, Birmingham, UK, 1995.
[28] N.M. Mahmoodi, Synthesis of amine-functionalized magnetic ferrite nanoparticle and its dye removal ability, J. Environ. Eng., 139 (2013) 1382–1390.
[29] N.M. Mahmoodi, A. Maghsoodi, Kinetics and isotherm of cationic dye removal from multicomponent system using the synthesized silica nanoparticle, Desal. Wat. Treat., 54 (2015) 562–571.
[30] G. Crini, P.M. Badot, Application of chitosan, a natural aminopolysaccharide, for dye removal from aqueous solutions by adsorption processes using batch studies: a review of recent literature, Prog. Polym. Sci., 33 (2008) 399–447.
[31] K. Sahithya, D. Das, N. Das. Adsorptive removal of monocrotophos from aqueous solution using biopolymer modified montmorillonite–CuO composites: equilibrium, kinetic and thermodynamic studies, Process Saf. Environ. Prot., 99 (2016) 43–54.
[32] N.M. Mahmoodi, Dendrimer functionalized nanoarchitecture: synthesis and binary system dye removal, J. Taiwan Inst. Chem. Eng., 45 (2014) 2008–2020.
[33] M.J. Temkin, V. Pyzhev, Recent modification to Langmiur isotherms, Acta Physiochim. USSR, 12 (1940) 217–222.
[34] N.M. Mahmoodi, Surface modification of magnetic nanoparticle and dye removal from ternary systems, J. Ind. Eng. Chem., 27 (2015) 251–259.